Metalloporphyrin Oligomers with Collapsible Cavities: Characterisation and Recognition Properties of Individual Atropisomers

Nick Bampos, Valérie Marvaud, and Jeremy K. M. Sanders*

Abstract: Hydrogenation of a butadiyne-linked cyclic porphyrin dimer and trimer leads to new tetramethylene-linked [-$(CH_2)_4$-] hosts. The flexible linkers give rise to multiple exchanging atropisomers of the trimer, and cavities that are collapsible. NMR spectroscopy has been used to characterise the equilibration and recognition properties of two of these individual trimer atropisomers: competition experiments with other trimers show that the all-*cis* isomer binds to *s*-tri(4-pyridyl)triazine with an affinity in $CDCl_3$ solution of 10^9–$10^{11}\,M^{-1}$; its cavity responds to the included ligand, to produce the optimum geometry for three simultaneous pyridine–Zn interactions. The *trans,trans,cis* isomer recognises 1,4-diazabicyclo[2.2.2]octane (DABCO) very efficiently by cofacial binding of two porphyrin units, forcing the third unit into a perpendicular geometry that leads to characteristic chemical shift effects extending over many Ångstroms. In each case, the added ligand binds sufficiently strongly to shift the atropisomer distribution quite dramatically. The corresponding dimer appears to be intramolecularly aggregated, significantly inhibiting intracavity binding; only DABCO is bound strongly within the cavity.

Keywords: atropisomerism · metalloporphyrins · molecular recognition · porphyrinoids · zinc

Introduction

One of the key aims of supramolecular chemistry is to create enzyme mimics capable of recognition and catalysis.[1] A key step of our research in this area was the controlled synthesis of the butadiyne-linked trimer [Zn_3(**1**)] and related dimers and tetramers by means of templated Glaser–Hay coupling of preformed porphyrin monomers, Equation (1).[2,3]

$$\text{Porph}{-}\text{C}{\equiv}\text{C}{-}\text{H} + \text{H}{-}\text{C}{\equiv}\text{C}{-}\text{Porph} \rightarrow \text{Porph}{-}\text{C}{\equiv}\text{C}{-}\text{C}{\equiv}\text{C}{-}\text{Porph} \quad (1)$$

This trimer has proved to be a versatile object for molecular recognition: it has well-defined ligand-binding properties,[4] stereoselectively accelerates an *exo*-Diels–Alder reaction,[5] and also catalyses an acyl transfer.[6] However, it has been an important part of our strategy to create a series of receptors using the same fundamental Zn–N recognition event, but with a range of cavity shapes and sizes, and preferably using the same diarylporphyrin monomer as a building block. In this paper we describe how the hydrogenation of the butadiyne linkers in trimer [Zn_3(**1**)] and dimer [Zn_2(**2**)] generates the tetramethylene-linked floppy trimer [Zn_3(**3**)] and floppy dimer [Zn_2(**4**)]. Unlike its parent [Zn_3(**1**)], the new trimer is ineffective at accelerating our Diels–Alder reaction because the Diels–Alder transition state is very well defined and so is sensitive to any changes in the geometry. As is often the case, these new hosts are shown to have cavities with geometrical and ligand-binding properties radically different from those of their parents that might have not been anticipated in the early stages of planning.[7]

[*] Prof. J. K. M. Sanders, N. Bampos, V. Marvaud
Cambridge Centre for Molecular Recognition
University Chemical Laboratory
Lensfield Road, Cambridge CB2 1EW (UK)
Fax: Int. code + (44) 1223 336017
e-mail: jkms@cam.ac.uk

Results and Discussion

Synthesis and characterisation of the nonrigid trimer: Hydrogenation of the (analytically pure) parent host [Zn_3(**1**)] with Pd/C in THF gave the new tetramethylene-linked host [Zn_3(**3**)] in good yield (>75%). Characterisation by mass spectrometry was straightforward and loss of the butadiyne UV absorptions at $\lambda = 315$–335 nm was also diagnostic. However, the ^{1}H NMR spectrum was extremely complex (Figure 1a), displaying a number of signals around $\delta = 10$ where a single *meso* resonance was expected. The spectrum of the free base H_6(**3**) was similar. The large number of signals and their differing intensities rule out the presence of only two conformers. This complexity persisted through many rounds of attempted purification by chromatography and recrystallisation, and we were eventually forced to accept that it is an intrinsic property of the pure compound. Furthermore,

  0947-6539/98/0402-0335 $ 17.50+.25/0

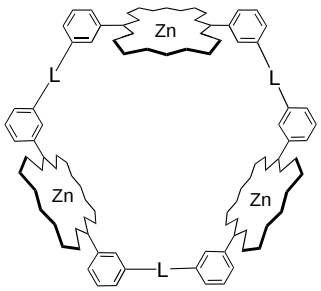

[Zn_3(**1**)] L = C≡C—C≡C
[Zn_3(**3**)] L = $(CH_2)_4$

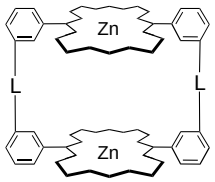

[Zn_2(**2**)] L = C≡C—C≡C
[Zn_2(**4**)] L = $(CH_2)_4$
[Zn_2(**6**)] L = C≡C

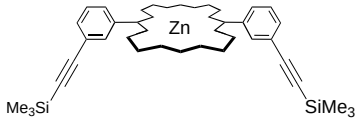

[Zn (**5**)]

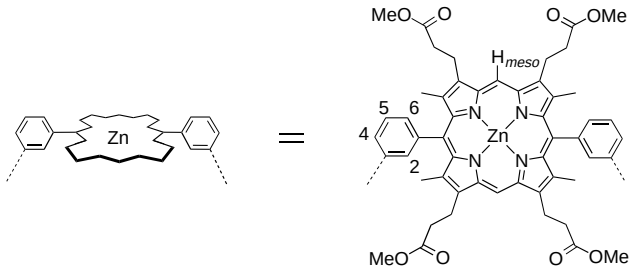

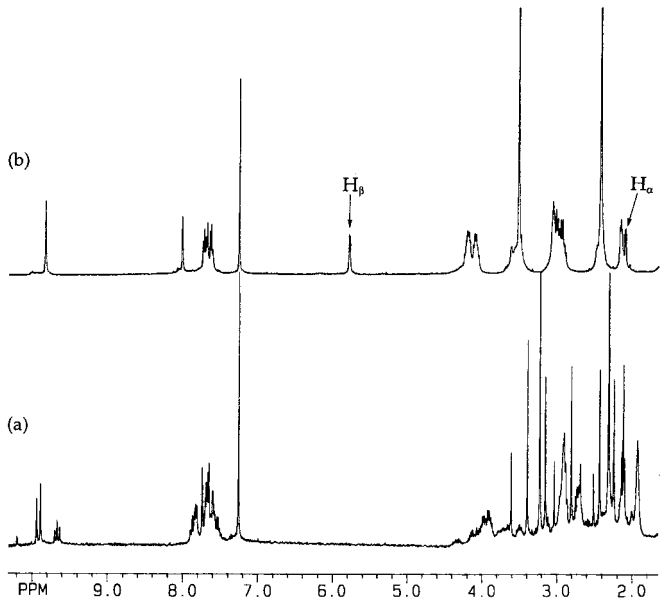

Figure 1. ^{1}H NMR spectrum (400 MHz, $CDCl_3$, 298 K) of a) [Zn_3(**3**)]; b) the same sample after addition of 1 equivalent of Py_3T.

neither the number nor the relative intensities of the signals were significantly dependent on temperature (320 to 220 K in $CDCl_3$) or concentration (10^{-3} to 10^{-5} M). The explanation must therefore lie in the presence of slowly exchanging atropisomers that differ in the *cis*/*trans* arrangement of the tetramethylene linkers.[4,8] This is confirmed by the simplification of the spectrum upon addition of the trifunctional ligand *s*-tri(4-pyridyl)triazine (Py_3T, Figure 1b). Scheme 1 shows three of the four possible conformational isomers, together with the major complexes with Py_3T and DABCO, which are described in more detail below.

COSY spectroscopy defined coupled sequences of protons in the ^{1}H NMR spectrum of ligand-free [Zn_3(**3**)]. Tight overlapping spin systems were identified in the aromatic region between $\delta = 7.5$ and 8.0, while more dispersed coupled partners were identified in the aliphatic region between $\delta = 1.9$ and 4.5 for the CH_2CH_2 fragments of the porphyrin ester side chains, in addition to the CH_2 groups of the tetramethylene linkers ($\delta \approx 3.0$ and 2.1). As many as six ester side-chain CH_2CH_2 pairs were assigned in the COSY spectrum, but could not be connected through spin coupling with the six isolated *meso* resonances. Other coupled spin systems might also have been present, but the low intensity of some resonances made identification of diagnostic cross-peaks in heavily congested regions difficult.

The NOESY spectrum was even more complicated but correspondingly more informative. Beginning with the resonances in the *meso* region, a series of porphyrin units were constructed from the NOE connectivities between *meso* resonance(s), the ester side chain(s), the methyl groups, the linker and aromatic protons (Scheme 2). In the case of a spatially symmetrical trimer, only resonances attributed to one such porphyrin unit might be expected, characterised by a single *meso* proton. For nonsymmetrical trimers, more than one porphyrin unit (and consequently more than one *meso* proton) would be expected for each cyclic oligomer, each unit connected to the others by the NOEs transmitted through the connecting tetramethylene linkers.

In the NOESY spectra of these large molecules, true NOE cross-peaks and those arising from chemical or conformational exchange appear with the same negative phase;

0947-6539/98/0402-0336 $ 17.50+.50/0 *Chem. Eur. J.* **1998**, *4*, No. 2

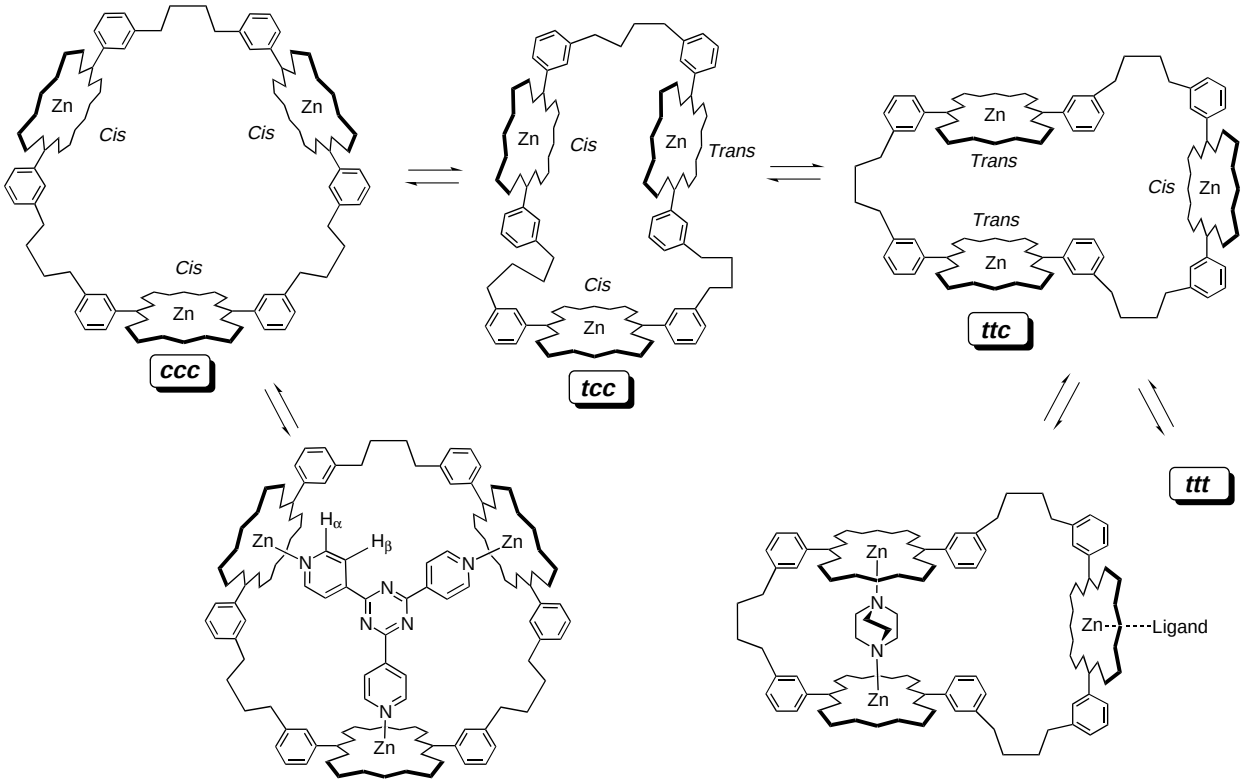

Scheme 1. Conformational isomers of $[Zn_3(\mathbf{3})]$ in solution and their major Py_3T and DABCO complexes. The isomerism is defined by the relative orientation of the alkyl chains linking any two porphyrins relative to the plane of the assigned porphyrin.

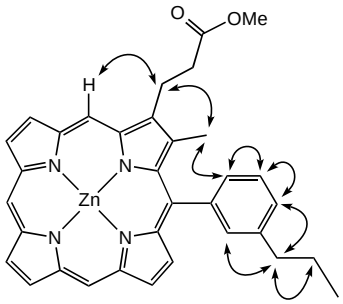

Scheme 2. Some intramolecular NOEs used to construct connectivities around a porphyrin ring.

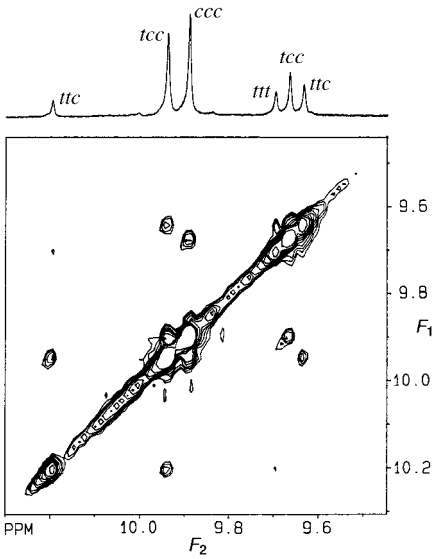

Figure 2. *Meso* region of the NOESY spectrum of $[Zn_3(\mathbf{3})]$ (500 MHz, $CDCl_3$, 300 K, $\tau_m = 900$ ms), showing exchange peaks between atropisomers.

however in ROESY spectra it proved easy to distinguish negative exchange peaks due to intermolecular exchange between specific *meso* protons of the various conformational forms from through-space NOE cross-peaks.[9] Similar exchange peaks were identified in the aromatic region and for sets of methyl and methoxy singlets in the aliphatic region. Inspection of the remote *meso* region of the ROESY (or NOESY) spectrum (Figure 2) shows exchange only between certain resonances. The resonance at $\delta = 9.88$, which had exchange cross-peaks only to the resonances at $\delta = 9.93$ and 9.66 (intensity ratio 2:1 respectively), was assigned to the open $[Zn_3(\mathbf{3})]$ form, on the basis that it displayed the simplest connectivity pattern to other resonances in the spectrum and its similarity to the $[Zn_3(\mathbf{3})(py_3t)]$ complex, described below.

The interconversion of the different forms of $[Zn_3(\mathbf{3})]$ requires that one porphyrin–aromatic bond is allowed to flip by 180°. Rotating one such bond of the *cis*,*cis*,*cis* (*ccc*) isomer will result in one *trans* porphyrin unit, while the other two will remain *cis*, forming the *trans*,*cis*,*cis* (*tcc*) conformer. This *tcc* atropisomer should give two *meso* resonances in the ratio 2:1, consistent with the experimental observation described above; this mechanism does not give rise to direct exchange peaks between inequivalent positions of the same isomer and,

significantly, no cross-peak was observed between the signals of the *tcc* atropisomer at $\delta = 9.93$ and 9.66.

In the NOESY spectrum, the two peaks attributed to the *tcc* atropisomer exhibit exchange peaks to the *ccc* atropisomer, in addition to resonances at $\delta = 10.19$ and 9.63 (ratio 1:2). No exchange peaks were identified between the two *meso* peaks at $\delta = 10.19$ and 9.63 and the *ccc meso* resonance at $\delta = 9.88$, or between the peaks at $\delta = 10.19$ and 9.63. This implies interconversion of a second *cis* porphyrin in the *tcc* form, into the *trans* geometry and a resulting *trans,trans,cis* (*ttc*) atropisomer. Both *meso* resonances of the *ttc* form exhibit exchange cross-peaks to the two peaks of the *tcc* atropisomer in addition to a small singlet at $\delta = 9.69$, which shows no cross-peak to any other *meso* peaks. It follows that the $\delta = 9.69$ peak be assigned to the all-*trans* (*ttt*) form. Relative intensities of the well-separated singlets give a *ccc*:*tcc*:*ttc*:*ttt* distribution of $\approx 22:25:9:4$, rather than the statistical 1:3:3:1 which would be expected in the absence of any strain. The *tcc* isomer is slightly more abundant than expected and *ccc* is the most favoured, while the *ttc* and *ttt* are clearly disfavoured to a small extent.

A similar series of exchange peaks were identified for the methoxy methyl and pyrrolic methyl resonances (to which indirect NOEs were recorded from the *meso* protons), which also helped in the assignment of many of the resonances of this complicated spectrum, and confirmed the presence of the various atropisomeric forms.

NMR titrations: tri-, bi- and monodentate nitrogen-based ligands

Characterisation of the Py_3T complex: The dramatically simpler spectrum (Figure 1b) of the $[Zn_3(\mathbf{3})(py_3t)]$ complex is similar to that of the rigid trimer $[Zn_3(\mathbf{1})]$ and its Py_3T complex;[3] it also confirmed the purity of $[Zn_3(\mathbf{3})]$. At room temperature, all signals associated with the Py_3T complex appear sharp; bound Py_3T signals appear at $\delta = 5.77$ (H_β) and 2.08 (H_α), significantly shifted to high field as a result of the porphyrin ring current. The complex is in slow exchange with excess ligand resonating at $\delta = 8.56$ and 8.93. Significantly, the bound Py_3T signals for the floppy trimer $[Zn_3(\mathbf{3})]$ were recorded at slightly higher field (by ≈ 0.1 and 0.3 ppm for H_β and H_α, respectively) relative to the $[Zn_3(\mathbf{1})]$ complex, owing to an increased ring current effect. This implies that the nonrigid trimer can contract into its own cavity so as to bind the Py_3T molecule more effectively. This result is consistent with modelling and experimental[10] studies, which indicate that Py_3T is slightly too small for the rigid $[Zn_3(\mathbf{1})]$ analogue, and with the competition experiments described below. COSY and NOESY spectra provided further structural characterisation of the $[Zn_3(\mathbf{1})(py_3t)]$ complex; Scheme 3 summarises the key host–guest cross-peaks observed in the NOESY spectrum. The ^{13}C NMR spectrum of $[Zn_3(\mathbf{3})(py_3t)]$ also became simplified and sharpened upon addition of Py_3T.

UV/Vis conformational analysis: The UV/Vis spectrum of $[Zn_3(\mathbf{3})]$ contains a broad Soret band at $\lambda = 411$ nm ($W_{1/2} \approx 17$ nm) in contrast to the corresponding peak for the rigid trimer $[Zn_3(\mathbf{1})]$ at $\lambda = 409$ nm ($W_{1/2} \approx 10$ nm). The breadth of the $[Zn_3(\mathbf{3})]$ Soret band may be due in part to the overlap of inequivalent bands from the various atropisomers and in part to exciton coupling between individual porphyrin units within some of the isomers;[11] the flexible linkers would allow favourable $\pi-\pi$-interactions and close porphyrin proximity as seen in some of our earlier systems.[12] Titration of a Py_3T/CH_2Cl_2 solution resulted in a lack of isosbesticity, but finally led to a sharp band, red-shifted by approximately 7 nm. Unfortunately, the complications of time-dependent atropisomerism and nonisosbesticity precluded any meaningful determination of binding constants.

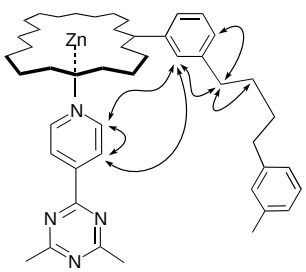

Scheme 3. Schematic representation of a fragment of the $[Zn_3(\mathbf{3})(py_3t)]$ complex, showing significant through-space connectivities from NOESY spectroscopy ($\tau_m = 1.2$ s), in addition to those shown in Scheme 2.

In order to probe the binding interaction in more detail, a millimolar Py_3T/CH_2Cl_2 solution (up to one equivalent) was added to a micromolar solution of $[Zn_3(\mathbf{3})]$ and the appearance of the Soret band in the UV/Vis spectrum was monitored as a function of time (spectrum recorded within four seconds of ligand addition, every second for up to two minutes). The intention was to observe slight changes in the appearance of the broad Soret band in the early stages after addition that might suggest a perturbation in the equilibrium of the atropisomers, but the changes at UV concentrations, if any, proved difficult to detect.

In a series of NMR competition experiments, the Py_3T complex of one trimer was formed (i.e. floppy $[Zn_3(\mathbf{3})]$ or rigid $[Zn_3(\mathbf{1})]$), and then an amount between 0.5 equiv and an excess of the other trimer added. In the ^1H NMR spectrum, the bound Py_3T H_β-protons of the two complexes $[Zn_3(\mathbf{1})(py_3t)]$ and $[Zn_3(\mathbf{3})(py_3t)]$, appearing at $\delta = 5.87$ and 5.77, respectively, were the most useful probe. After some hours, equilibrium was reached, with Py_3T distributed between $[Zn_3(\mathbf{1})]$ and $[Zn_3(\mathbf{3})]$ in a ratio of approximately 35:65. When the same experiments were repeated in the presence of three equivalents of pyridine, the final equilibrium—again reached after some hours—favoured the $[Zn_3(\mathbf{3})(py_3t)]$ complex over the $[Zn_3(\mathbf{1})(py_3t)]$ complex by 7:1; selected spectra from the titration are shown in Figure 3. These experiments show a) that Py_3T has an intrinsic binding constant for *ccc*-$[Zn_3(\mathbf{3})]$ that is larger than for the rigid $[Zn_3(\mathbf{1})]$ ($\approx 10^9\,M^{-1}$); b) that interconversion between the atropisomers followed by trapping of *ccc* with Py_3T is a slow process, taking some hours to reach equilibrium; c) that in the absence of added pyridine, there are probably intramolecular $\pi-\pi$-interactions within some of the atropisomers, reducing the affinity for free ligands.[12] The large affinity of *ccc*-$[Zn_3(\mathbf{3})]$ for Py_3T, deduced from these competition experiments, is consistent with the cavity contraction and close porphyrin–ligand approach indicated by the chemical shifts of the bound ligand. On

0947-6539/98/0402-0338 $ 17.50+.50/0 *Chem. Eur. J.* **1998**, *4*, No. 2

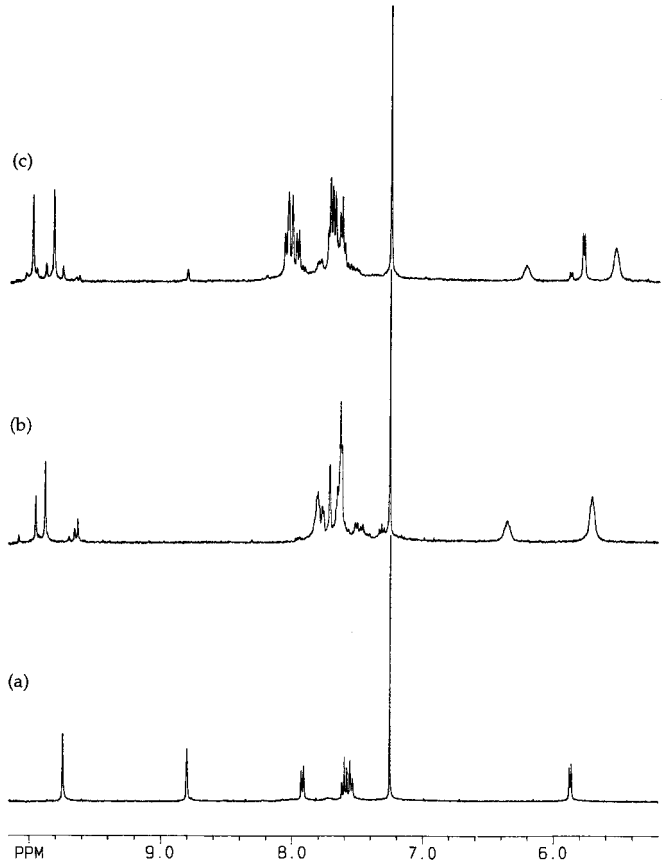

Figure 3. ^{1}H NMR spectrum (400 MHz, $CDCl_3$, 298 K) of a) 1 equiv Py_3T added to a 2.2.2 rigid trimer [Zn_3(**1**)] solution; b) 3 equiv pyridine added to 1 equiv of the floppy trimer [Zn_3(**3**)]; c) the spectrum resulting from the addition of b) to a). The sample was monitored over two weeks, showing little change in appearance relative to that acquired soon after addition.

addition of the rigid trizinc trinitro- or hexanitro trimers to a solution of [Zn_3(**3**)(py_3t)], the ligand migrated exclusively to the strongly-binding nitro trimers, so its affinity for [Zn_3(**3**)] is less than $\approx 10^{11}\,\mathrm{M}^{-1}$.[2,13]

Characterisation of the 1:1 DABCO complex: A DABCO solution (millimolar in $CDCl_3$) was titrated into a [Zn_3(**3**)] solution and changes in the appearance of the ^{1}H NMR spectrum were recorded. Less than one added equivalent afforded a sharp resonance at $\delta = -5.25$, diagnostic of the bidentate guest doubly bound inside the cavity and, as a result, experiencing the ring current of two neighbouring porphyrin rings.[10] While the aliphatic region of the spectrum was simplified relative to the initial [Zn_3(**3**)] spectrum, a number of *meso* resonances were still observed in the lowfield region, with the aromatic region containing a complex overlay of signals extending to $\delta = 6.9$. One equivalent of added DABCO gave a sharp *meso* peak at $\delta = 9.43$ and two low intensity, broad resonances at $\delta = 10.4$ and 9.9, with only a slight further simplification in the appearance of the aromatic and aliphatic regions. The signal at $\delta = 9.4$ is characteristic of the mutual upfield shift experienced by two porphyrins bound to a single DABCO molecule.[12]

Addition of up to four equivalents of DABCO to the [Zn_3(**3**)] solution produced a sharp and radically different spectrum. While the high-field resonance at $\delta = -5.25$ broadened significantly, sharp aromatic resonances were identified, particularly at $\delta = 6.84$ (d), 6.73 (d) and 6.31 (dd). The *meso* region contained three identifiable resonances: two singlets at $\delta = 10.27$ and 9.48 in a ratio 1:2, which are attributed to a single trimer molecule, plus a less intense singlet at $\delta = 9.87$, attributed to a symmetrical trimer. The first and major species incorporates a DABCO molecule bound between two porphyrin rings, with a second ligand bound on the exterior face of the third porphyrin (Scheme 1) acting as a monodentate ligand capping the third porphyrin, or as a bidentate ligand bringing together two 1:1 complexes to form a dimer of trimers (overall 2 *meso* signals in ratio 1:2 would be expected). The minor symmetrical species is attributed to [*ccc*·(dabco)$_3$], with a monodentate ligand at each porphyrin ring. The many other different DABCO-bound oligomers that may be envisaged are present in concentrations too low to be significant.

The 1:1 DABCO–trimer sandwich complex has one free binding site. Addition of quinuclidine (one equivalent) gave rise to two additional broad peaks at $\delta = -0.4$ and -2.7; these shifts are similar to those obtained from NMR titrations of quinuclidine with the monomer [Zn(**5**)], and are consistent with binding to the exterior face of the third porphyrin.

When a large excess of DABCO was added (>10 equiv), the symmetrical [*ccc*·(dabco)$_3$] increased in abundance, and small peaks appeared at $\delta = 9.64$ and 9.23 (ratio 1:2), due to a new species that was not further characterised, but the sandwich complex remained dominant. This demonstrates the large effective molarity for intramolecular binding that is possible when the linkages are flexible.

Structural characterisation of the [Zn_3(**3**)(dabco)] complexes required the use of two-dimensional NMR spectroscopy. COSY, NOESY and ROESY spectra were acquired of a [Zn_3(**3**)] solution containing four equivalents of DABCO, as the resonances, particularly the aromatic resonances between $\delta = 8.2$ and 6.3, were sharp enough to resolve couplings, while the two complexes present were observed in spectroscopically measurable quantities. In addition, the unprecedented dispersion of the aromatic region allowed complete assignment of the spin-coupled systems by means of DQF COSY. Figure 4 shows a portion of the COSY spectrum containing the coupled protons of three unique aromatic rings of the dominant complex, while other coupled resonances were identified in the aliphatic region for methylene protons of the side chains and the methylene protons of the linkers.

NOESY and ROESY spectra allowed the identification of numerous NOEs and exchange peaks, leading to complete assignment of a number of species in solution. Diagnostic regions of the NOESY spectrum are shown in Figure 5. Some of the key connections illustrated in Scheme 4, together with model building, confirmed that the *ttc* complex is the major species in solution (assignment of resonances is summarised in Table 1): the shift to unusually high field of the two aromatic doublets [$\delta = 6.84$ (H_4^{II}) and 6.73 (H_6^{II})] and doublet of doublets [$\delta = 6.31$ (H_5^{II})] are due to the ring current of the third porphyrin ring. In addition to NOESY cross-peaks, H_4^{II} gives exchange cross-peaks to H_4^{I} and H_4^{III}, indicating fast

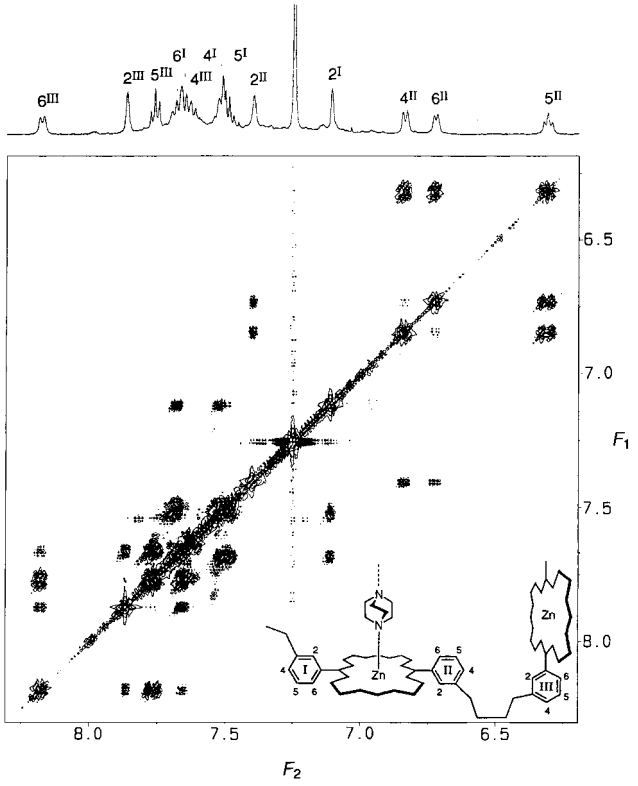

Figure 4. Aromatic region of the gradient-COSY spectrum (500 MHz, $CDCl_3$, 300 K, magnitude mode) of the [Zn_3(**3**)(dabco)] complex.

Table 1. Assignment of the proton resonances (δ) of the [Zn_3(**3**)(dabco)] complex shown in Scheme 4.

	Fragment I	Fragment II	Fragment III
meso-H	9.48	9.48	10.27
-Me	2.15	1.87	2.63
-OMe	3.44	3.40	3.74
-CH_2CH_2COOMe	2.72	2.68	3.30
-CH_2CH_2COOMe	4.05	3.90	4.50
-H2	7.11	7.40	7.87
-H4	7.52	6.84	7.65
-H5	7.62	6.31	7.76
-H6	7.69	6.73	8.17
Ph-CH_2CH_2-	2.89	2.73	3.05
Ph-CH_2CH_2-	1.93	1.89	1.88

conformational exchange of the 1:1 complex on the T_1 timescale. A similar series of NOESY and exchange cross-peaks can be assigned for each of the other aromatic protons, the methyl and methoxy singlets. The DABCO resonance at $\delta = -5$ is significantly exchange-broadened and no cross-peaks can be identified between it and the sharp resonances of the host. The third porphyrin may use an additional DABCO molecule to bind to a second *ttc*·dabco trimer complex. The spectra also confirmed the structure of the minor [*ccc*·(dabco)$_3$] complex to be similar to the Py_3T complex.

Other monodentate and bidentate ligands: Addition of up to 3 equiv pyridine or quinuclidine to a $CDCl_3$ solution of [Zn_3(**3**)] resulted in a slight change in the appearance of the spectrum, although a complex *meso* region was still observed.

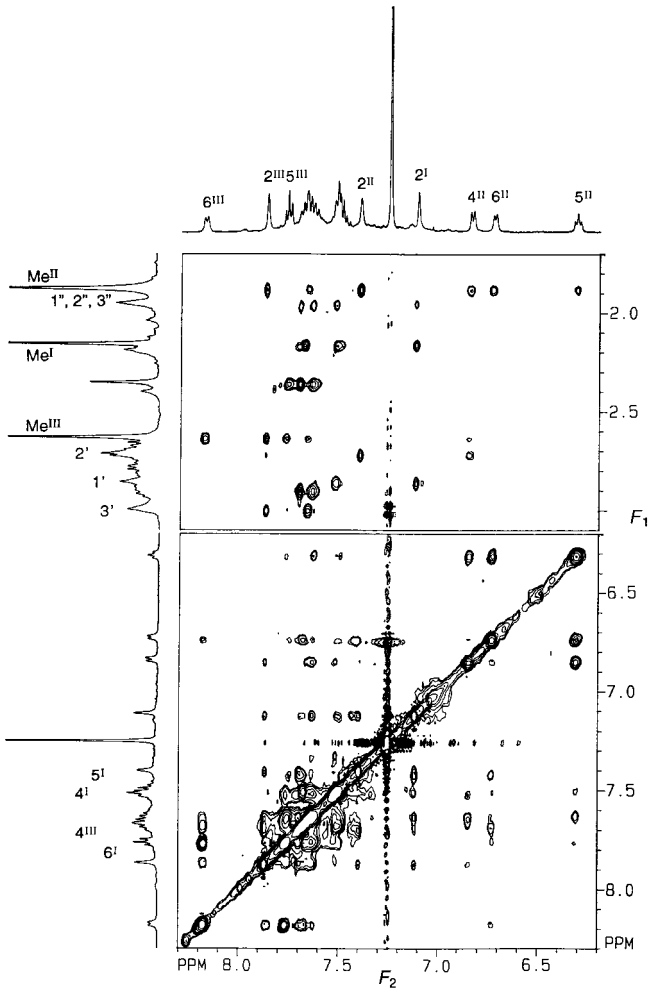

Figure 5. Selected region of the NOESY spectrum (500 MHz, $CDCl_3$, 300 K, $\tau_m = 900$ ms) for the [Zn_3(**3**)(dabco)] complex (ratio 1:4). Significant cross-peaks (through space) are observed between the 4^{II} aromatic proton and 2′, Me^{III} and 2^{III}.

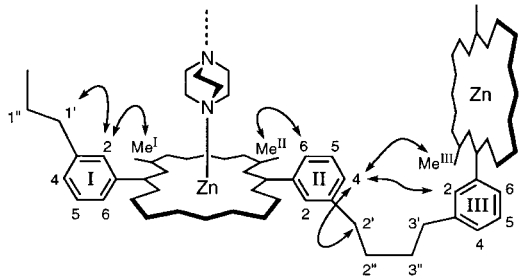

Scheme 4. Through-space connectivities for the [Zn_3(**3**)(dabco)] complex observed in the NOESY spectrum (500 MHz, $CDCl_3$, 300 K, $\tau_m = 900$ ms).

Broad resonances for bound pyridine appeared at $\delta = 6.3$ (H_γ, $\Delta\delta = -1.3$) and 5.6 (H_β, $\Delta\delta = -1.6$) as expected, while the most dramatically affected third resonance ($\delta = H_\alpha$, $\Delta\delta \approx -6$) was buried in the congested aliphatic region. Binding quinuclidine to each monomer of the trimer, gave identifiable highfield resonances at $\delta = -3.35$ ($\Delta\delta = -6.19$) and -0.59 ($\Delta\delta = -2.11$), in addition to a resonance in the aliphatic region at $\delta \approx 1.60$ ($\Delta\delta = -0.13$). This behaviour parallels that

0947-6539/98/0402-0340 $ 17.50+.50/0 *Chem. Eur. J.* **1998**, *4*, No. 2

for the addition of ligands to monomers. More than three equivalents of added ligand gave resonances for the ligand as an average between the bound and unbound chemical shifts, but the *meso* region remains complicated with at least four identifiable resonances. It appears, therefore, that monodentate ligands are unable to change the atropisomeric equilibrium dramatically.

A series of bidentate guests was also investigated: 4,4′-bipyridyl, BiPy; 1,2-bis(4-pyridyl)ethane, Py_2Et; 1,3-bis(4-pyridyl)propane, Py_2Pr; and 4′-phenyl-4,2′:6′,4″-terpyridyl, Py_2Py. To varying degrees, these behaved in ways that were intermediate between monodentate ligands and Py_3T. In no case was it possible to characterise precise geometries.

Synthesis and characterisation of the floppy dimer: The ^{1}H NMR spectrum of the rigid dimer [Zn_2(**2**)] exhibits sharp resonances for all the proton environments over a range of temperatures and solvents, while the UV spectrum gives a sharp Soret band at $\lambda = 410$ nm.[2] Hydrogenation of the bisacetylene linkers gave a product ([Zn_2(**4**)]) in high yields ($>$ 85 %) and which was pure by tlc; the ^{1}H NMR spectrum gave broad aromatic and aliphatic resonances and a *meso* resonance that was too broad to define, while in the UV/Vis spectrum the Soret band was blue-shifted to $\lambda = 406$ nm. These properties are characteristic of intramolecularly π-stacked porphyrins.[11,12] Changing the solvent or the temperature at which spectra were acquired had no significant effect on the appearance of the NMR spectrum. Demetallation of [Zn_2(**4**)] (by treatment with 5 % TFA in methanol) afforded a sharp ^{1}H NMR spectrum for H_4(**4**), with a single *meso* resonance at $\delta = 8.95$. Spectra acquired at temperatures as low as 210 K in $CDCl_3$ were highly broadened and resembled those of the metallated analogues at ambient temperature. This behaviour is entirely consistent with the greater π-stacking tendency of metallated porphyrins.[14] The dimer does not have sufficient flexibility to exhibit atroposomerism, and has therefore a simpler complexation chemistry.

NMR titrations with amines: Addition of less than one equivalent of quinuclidine or pyridine to a solution of [Zn_2(**4**)] in no produced no significant sharpening of the porphyrin resonances, and resulted in the appearance of bound ligand signals, as usual. When more than one equivalent of ligand was added, the porphyrin signals sharpened and were simplified considerably, while the ligand resonances broadened into the baseline. This behaviour is similar to that of earlier floppy dimers exhibiting intramolecular aggregation.[12] The *meso* resonance appeared at $\delta \approx 9.6$, upfield shifted by ≈ 0.4 ppm due to intramolecular ring current effects. This effect of neighbouring porphyrins is confirmed by careful addition of [Zn(**5**)] to a DABCO solution. When one equivalent of monomer was added, the *meso* proton shifts from $\delta = 10.21$ to 10.08, while addition of a second equivalent of the monomer shifts the *meso* resonance further upfield ($\delta \approx 9.7$) due to the formation of the ternary complex (Scheme 5, (a)). In this case, the porphyrin–porphyrin distance is dependent on the ligand and the natural nitrogen–zinc bond length, with no additional structural constraints inherent in both cyclic dimer hosts. Similar shift effects are apparent in the DABCO and BiPy complexes of [Zn_2(**4**)] and [Zn_2(**2**)] and [Zn_2(**6**)][15] (Scheme 5).

NMR competition experiments between [Zn_2(**4**)] and [Zn_2(**2**)] with various ligands gave results which are consistent with the guest binding to the best-fit host. Addition of one equivalent of the nonrigid host [Zn_2(**4**)] to a solution of the [Zn_2(**2**)(bipy)] complex afforded no change in the appearance of the spectrum, while addition of [Zn_2(**4**)] to a 1:1 mixture of [Zn_2(**2**)] and DABCO resulted in the formation of the [Zn_2(**4**)(dabco)] complex with free [Zn_2(**2**)]. Furthermore, addition of DABCO or BiPy to a 1:1 mixture of dimers [Zn_2(**2**)] and [Zn_2(**4**)] gave exclusively spectra for the [Zn_2(**4**)(dabco)] and [Zn_2(**2**)(bipy)] complexes, respectively, with the accompanying free host.

Conclusions

The design strategy leading to porphyrin trimer [Zn_3(**1**)] called for rigid linkers to separate the various ligand binding sites and create large open cavities.[2,3] This strategy was partially the result of earlier experiences with the collapsed cavities of flexibly-linked cofacial porphyrin dimers.[12] In this paper we have shown that hydrogenation of the rigid butadiyne linkages in [Zn_3(**1**)] leads to a situation that can be portrayed either as hopelessly complex or as extremely rich in information. Using modern NMR techniques to probe the processes occurring in an equilibrium mixture, we have characterised the structures and dynamic interconversion of several atropisomers and demonstrated the very different molecular recognition properties of two of these isomers. The all-*cis* isomer binds to Py_3T with an affinity that exceeds the 10^9 M^{-1} of [Zn_3(**1**)] but is less than 10^{11} M^{-1}; its cavity responds

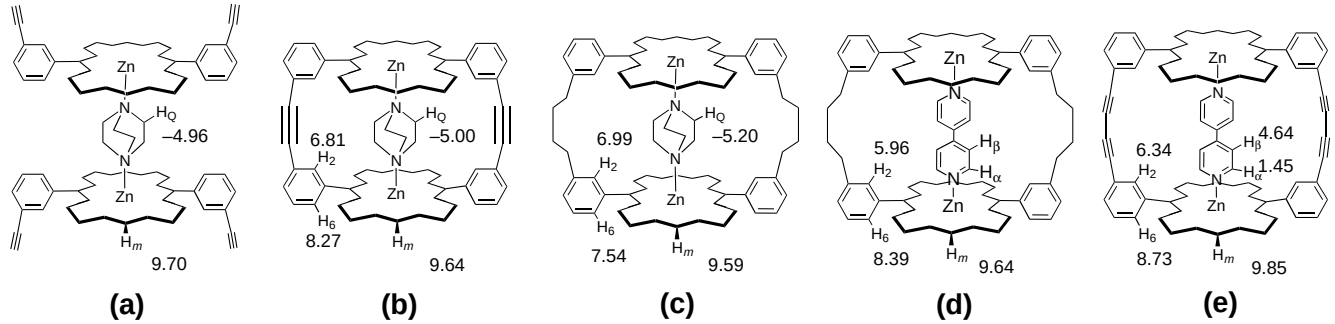

Scheme 5. Comparative chemical shifts for DABCO and BiPy complexes of [Zn(**5**)] (a), [Zn_2(**6**)] (b), [Zn_2(**4**)] (c, d) and [Zn_2(**2**)] (e).

to the included ligand, giving the optimum geometry for three simultaneous pyridine–Zn interactions. In contrast, the *trans,trans,cis* isomer recognises DABCO very efficiently by cofacial binding of two porphyrin units, forcing the third unit into a perpendicular geometry that leads to characteristic chemical shift effects extending over many Ångstroms. In each case, the added ligand binds sufficiently strongly to shift the atropisomer distribution quite dramatically. The corresponding floppy dimer [Zn_2(**4**)] appears to be intramolecularly aggregated to a considerable extent, significantly inhibiting intracavity binding; only DABCO possesses the correct geometry and binding strength to be bound strongly within the cavity.

Experimental Section

^{1}H NMR spectra were recorded on Bruker DPX 250 MHz, AM 400 MHz or DRX 500 MHz spectrometers. Unless otherwise stated, spectra were acquired in $CDCl_3$ at 300 K and referenced relative to solvent residuals ($\delta = 7.25$ for $CHCl_3$). For NMR titrations, the porphyrin solutions, typically $\approx 10^{-3}$ M in porphyrin, were acquired with spectral widths large enough to accommodate highfield resonances due to bound ligands. The chloroform used was passed through a short alumina column to remove water, but otherwise used as purchased.

UV/Vis spectra were recorded on a Hewlett Packard 8452 Å diode array spectrometer with temperature-regulated cell holders. Porphyrin solutions were prepared in dry CH_2Cl_2 (refluxed over K_2CO_3) and concentrations were typically $\approx 10^{-6}$ M in porphyrin.

Two-dimensional spectra (gradient DQF COSY, NOESY with 900 ms mixing time and ROESY with a 600 ms spinlock pulse, from standard Bruker pulse programs) were acquired at 300 K with a relaxation delay of 2 s and 2048 data points in t_2. Typically, 16 scans were accumulated for 640 increments in t_1. Prior to FT, zero filling was applied to both t_2 and t_1 (1 K) and the data multiplied by a shifted sine-bell function in both domains.

DABCO, quinuclidine, BiPy, Py_2Et and Py_2Pr were purchased from Aldrich and sublimed prior to use. Py_2Py[16] and Py_3T[4,17] were prepared according to reported methods. Liquid ligands were used as purchased, while protonated solvents were distilled over a suitable drying agent prior to use. $CDCl_3$ was passed through a short alumina plug to remove moisture and traces of acid.

Floppy dimer [Zn_2(4)]: The rigid dimer [Zn_2(**2**)] (150 mg, 0.077 mmol) was dissolved in dry THF (400 mL, sparingly soluble), Pd/C catalyst added (0.7 g) and the mixture stirred overnight under H_2 (three pump/H_2 cycles). The mixture was filtered (Celite) and the solvent evaporated. The red product was chromatographed on silica gel with $CHCl_3$ and subsequently recrystallised from $CHCl_3$/MeOH. Yield 135 mg (89%). ^{1}H NMR (400 MHz, [D_5]pyridine): $\delta = 1.77$ (br t, 8H, -CH_2CH$_2$Ph), 2.24 (s, 24H, pyrrole CH_3), 2.71 (br t, 8H, -CH$_2$CH_2Ph), 2.88 (t, 16H, -CH$_2$CH_2COOCH$_3$), 3.43 (s, 24H, -CH$_2$CH$_2$COOCH_3), 4,08–3.99 (m, 16H, -CH_2CH$_2$COOCH$_3$), 6.93 (s, 4H, aryl CH_2), 7.51 (d, 4H, aryl CH), 7.57 (t, 4H, aryl CH), 8.01 (d, 4H, aryl CH), 9.65 (s, 4H, *meso-H*); ^{13}C NMR (100 MHz, [D_5]pyridine): $\delta = 14.9$ (*C*H$_3$), 21.6 (side-chain *C*H$_2$), 31.1, 35.4 (linker *C*H$_2$), 36.9 (side-chain *C*H$_2$), 51.3 (O*C*H$_3$), 96.2 (*meso-CH*), 118.9 (*meso-C*), 127.0, 127.8, 130.3, 133.4, 141.8, 143.5 (aryl *C*), 138.4, 140.4, 145.2, 147.2 (pyrrole *C*), 173.4 (*C*O); FAB calcd for $C_{112}H_{116}N_8O_{16}Zn_2$ 1961 [M^+], found 1959; UV/Vis (CH_2Cl_2): $\lambda_{max} = 407$ (Soret), 544, 577 (Q bands), 335 (broad) nm.

Floppy dimer H_4(4): [Zn_2(**4**)] (150 mg, 0.0765 mmol) was dissolved in CH_2Cl_2 (150 mL) and treated with trifluoroacetic acid (2×100 mL, methanolic solution). The resulting green solution was washed with water (5×300 mL), dried (over K_2CO_3), filtered and the solvent evaporated. The red product was chromatographed on silica gel with $CHCl_3$ and recrystallized from $CHCl_3$/MeOH. Yield 122 mg (87%). ^{1}H NMR (250 MHz, $CDCl_3$): $\delta = -3.19$ (s, 4H, inner protons), 2.01 (br t, 8H, -CH_2CH$_2$Ph), 2.29 (s, 24H, pyrrole CH_3), 2.70 (t, 16H, -CH$_2$CH_2COOCH$_3$), 2.95 (br t, 8H, -CH$_2$CH_2Ph), 3.53 (s, 24H, -CH$_2$CH$_2$COOCH_3), 3.59–3.41 (dq, 16H, -CH_2CH$_2$COOCH$_3$), 7.80–7.38 (m, 16H, aryl CH), 8.95 (s, 4H, *meso-H*); FAB calcd for $C_{112}H_{120}N_8O_{16}$ 1834.2 [M^+], found 1834; UV/Vis (CH_2Cl_2): $\lambda_{max} = 402$ (Soret), 507, 540, 575 (Q bands) nm.

Typical floppy dimer complex: The preparation of complexes of [Zn_2(**4**)], involved the titration of a ligand solution of known concentration into an NMR tube containing the porphyrin ($CDCl_3$) solution, also of known concentration. The ^{1}H NMR data for the BiPy complex presented below differs only slightly in the chemical shifts from the data for other bidentate guest–host complexes. Changes in the chemical shift of the 1:1 complex and the solution containing an excess of ligand are diagnostic for the change in the shape of the cavity and the influence of the resulting ring currents.

1:1 Complex: ^{1}H NMR (400 MHz, $CDCl_3$): $\delta = 1.33$ (m, 8H, -CH_2CH$_2$Ph), 2.27 (m, 8H, -CH$_2$CH_2Ph), 2.33 (s, 24H, pyrrole CH_3), 2.92 (m, 16H, -CH$_2$CH_2COOCH$_3$), 3.51 (s, 36H, -CH$_2$CH$_2$COOCH_3), 3.97, 4.19 (m, 16H, -CH_2CH$_2$COOCH$_3$), 5.92 (br s, 4H, aryl C*H2*), 7.38 (d, J(H4, H5) = 8.3 Hz, 4H, aryl C*H4*), 7.61 (dd, J(H5, H6) = 8.3 Hz, 4H, aryl C*H5*), 8.45 (br d, 4H, aromatic C*H6*), 9.69 (s, 4H, *meso*-H). Bound BiPy resonances not identified.

Excess ligand: ^{1}H NMR (400 MHz, $CDCl_3$): $\delta = 1.46$ (m, 8H, -CH_2CH$_2$Ph), 2.32 (s, 24H, pyrrole CH_3), 2.42 (m, 8H, -CH$_2$CH_2Ph), 2.92 (m, 16H, -CH$_2$CH_2COOCH$_3$), 3.49 (s, 36H, -CH$_2$CH$_2$COOCH_3), 3.96, 4.12 (m, 16H, -CH_2CH$_2$COOCH$_3$), 6.28 (s, 4H, aryl C*H2*), 7.43 (d, J(H4, H5) = 8.3 Hz, 4H, aryl C*H4*), 7.61 (dd, J(H5, H6) = 8.3 Hz, 4H, aryl C*H5*), 8.45 (d, 4H, aryl C*H6*), 9.64 (s, 4H, *meso*-H). Bound BiPy resonances not identified.

Floppy trimer, [Zn_3(**3**)]: The rigid trimer [Zn_3(**1**)] (44 mg, 0.015 mmol) was dissolved in dry THF (150 mL). Pd/C catalyst was added (0.3 g) and the mixture stirred overnight under H_2 (three pump/H_2 cycles). The solution was filtered (Celite) and the solvent evaporated. The pink product was chromatographed on silica gel with $CHCl_3$ and subsequently recrystallised from $CHCl_3$/MeOH. Yield 35 mg (79%). Characterised as the Py_3T adduct: ^{1}H NMR (400 MHz, $CDCl_3$): $\delta = 2.09$ (d, 6H, Py_3T H_α), 2.15 (br t, 12H, -CH_2CH$_2$Ph), 2.42 (s, 36H, pyrrole CH_3), 2.95 (t, 24H, -CH$_2$CH_2COOCH$_3$), 3.05 (br t, 12H, -CH$_2$CH_2Ph), 3.51 (s, 36H, -CH$_2$CH$_2$COOCH_3), 4.18 (m, 24H, -CH_2CH$_2$COOCH$_3$), 5.79 (d, 6H, Py_3T-H_β), 7.65 (m, 18H, aryl CH), 8.01 (s, 6H, aryl CH), 9.82 (s, 6H, *meso*-H); ^{13}C NMR (100 MHz, $CDCl_3$): $\delta = 15.0$ (*C*H$_3$), 22.0 (side-chain *C*H$_2$), 33.0, 36.6 (linker *C*H$_2$), 37.0 (side-chain *C*H$_2$), 51.5 (O*C*H$_3$), 96.3 (*meso-CH*), 119.4 (*meso-C*), 119.9 (Py_3T-C_β), 127.6, 128.5, 130.7, 133.3 (aryl *CH*), 138.5 (pyrrole *C*), 140.1 (Py_3T *C*), 140.8 (pyrrole *C*), 141.8 (aryl *C*), 143.7 (Py_3T *C*), 143.9 (aryl *C*), 145.5, 147.5 (pyrrole *C*), 168.6 (Py_3T *C*), 173.6 (*C*O); FAB calcd for $C_{168}H_{174}N_{12}O_{24}Zn_3$ 2941.5 [M^+], found 2940; UV/Vis (CH_2Cl_2): $\lambda_{max} = 411$ (Soret), 541, 575 (Q bands), 332 (broad) nm.

Acknowledgements: We thank the EPSRC (N.B.) and EC Human Capital and Mobility Programme (V.M.) for financial support, the SERC/EPSRC Mass Spectrometry Service in Swansea for mass spectra and Dr. D. McCallien for samples of the nitro-substituted porphyrins.

Received: July 21, 1997 [F772]

[1] For example, see: A. J. Kirby, *Angew. Chem.* **1996**, *108*, 770; *Angew. Chem. Int. Ed. Engl.* **1996**, *35*, 707; D. H. Kim, *Comprehensive Supramolecular Chemistry*, *Vol. 4* (Eds: J. L. Atwood, J. E. D. Davies, D. D. MacNicol, F. Vögtle), **1994**, Elsevier, 503–526.

[2] J. K. M. Sanders, *Comprehensive Supramolecular Chemistry*, *Vol. 9* (Eds.: J. L. Atwood, J. E. D. Davies, D. D. MacNicol, F. Vögtle), **1996**, Elsevier, 131–164.

[3] H. L. Anderson, J. K. M. Sanders, *J. Chem. Soc. Perkin Trans I* **1995**, 2223; S. Anderson, H. L. Anderson, J. K. M. Sanders, *J. Chem. Soc. Perkin Trans I* **1995**, 2247.

[4] H. L. Anderson, S. Anderson, J. K. M. Sanders, *J. Chem. Soc. Perkin Trans I* **1995**, 2231.

[5] C. J. Walter, J. K. M. Sanders, *Angew. Chem.* **1995**, *107*, 223; *Angew. Chem. Int. Ed. Engl.* **1995**, *34*, 217.

[6] L. G. Mackay, R. S. Wylie, J. K. M. Sanders, *J. Am. Chem. Soc.* **1994**, *116*, 3141.

[7] N. M. Glagovich, T. H. Webb, H. Suh, S. Geib, C. G. Wilcox, *Proc. Indian Acad. Sci. (Chem. Sci.)* **1994**, *106*, 955.

  0947-6539/98/0402-0342 $ 17.50+.50/0

[8] V. Marvaud, A. Vidal-Ferran, S. J. Webb, J. K. M. Sanders, *J. Chem. Soc. Dalton Trans* **1997**, 985; A. Vidal-Ferran, N. Bampos, J. K. M. Sanders, *Inorg. Chem.* **1997**, *36*, 6117.
[9] D. Neuhaus, M. P. Williamson, *The Nuclear Overhauser Effect in Structural and Conformational Analysis*, VCH, Cambridge, **1989**; J. K. M. Sanders, B. K. Hunter, *Modern NMR Spectroscopy*, 2nd ed., Oxford University Press, **1993**.
[10] A. Vidal-Ferran, C. M. Müller, J. K. M. Sanders, *J. Chem. Soc. Chem. Commun.* **1994**, 2657.
[11] C. A. Hunter, J. K. M. Sanders, A. J. Stone, *Chemical Physics* **1989**, *133*, 395.
[12] C. A. Hunter, M. N. Meah, J. K. M. Sanders, *J. Am. Chem. Soc.* **1990**, *112*, 5773; H. L. Anderson, C. A. Hunter, M. N. Meah, J. K. M. Sanders, *ibid.* **1990**, *112*, 5780.
[13] D. W. J. McCallien, J. K. M. Sanders, *J. Am. Chem. Soc.* **1995**, *117*, 6611; and unpublished results.
[14] C. A. Hunter, J. K. M. Sanders, *J. Am. Chem. Soc.* **1990**, *112*, 5525.
[15] A. Vidal-Ferran, Z. Clyde-Waston, N. Bampos, J. K. M Sanders, *J. Org. Chem.* **1997**, *62*, 240.
[16] F. Kröhnke, *Synthesis* **1976**, 1.
[17] H. Biedermann, K. Wichmann, *Naturforsch. Teil B* **1974**, *29*, 360.